Electronic Supplementary Material (ESI) for Soft Matter.

Supplementary Information

The fractal geometry of polymeric materials surfaces: Surface area and fractal length scales

(1) Structural Analysis of Polymeric Surfaces

The following AFM setting parameters were chosen for the present work:

- Tapping mode in air.
- SSS (super-sharp) tip (2 nm nominal tip radius).
- Nominal resonance frequency of 320 kHz , in the range (250-390) kHz, was used.
- Line scan frequency 0.3-0.5 Hz.
- Resolution of 512 pixel per line.

AFM tapping mode is used to scan all samples with a super-sharp tip capable of lateral resolution of about 2 nm. Tapping mode intermittent tip-sample contact reduces the lateral tip-sample force interactions and avoids probe-induced damage in soft surfaces (e.g. polymers). 2D scans, of both relative amplitude and topographic signals, for the samples examined in this paper are shown below. The images do not show clear evidence of artefacts caused by the probe nor by the probe-surface interactions. Open-source Gwyddion Data Analysis Software is used to remove scanner-induced artefacts.

(1.1) Polypropylene (PP)

Figure S1a,b show a typical PP sample studied in this work, at two different length scales. The original PP surface before treatment, here referred to as non-treated (NT) PP surface, and denoted as PP (NT), displays a root-mean-square (RMS) roughness of about 5 nm. Figure S1a shows both the 2D (upper panels) and 3D (lower panels) images. Figure S1b shows two arbitrary line profiles (lower panels).

The plasma treated counterparts to the PP samples shown in Figures S1a and S1b, denoted as PP (PT), are displayed in Figures S2a and S2b. Now the PP (PT) RMS roughness grows up to about 30 nm.

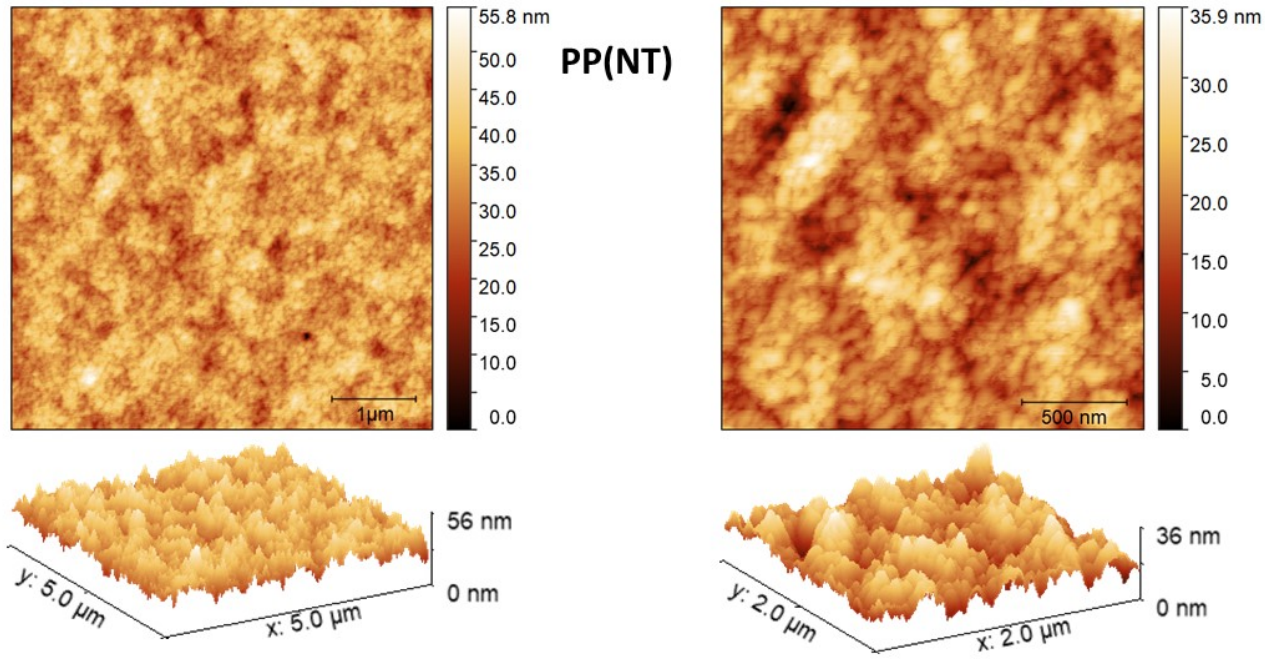

Figure S1a: The upper panels show the 2D (topographic) images for PP (NT) at two different scales. The lower panels display the corresponding 3D images.

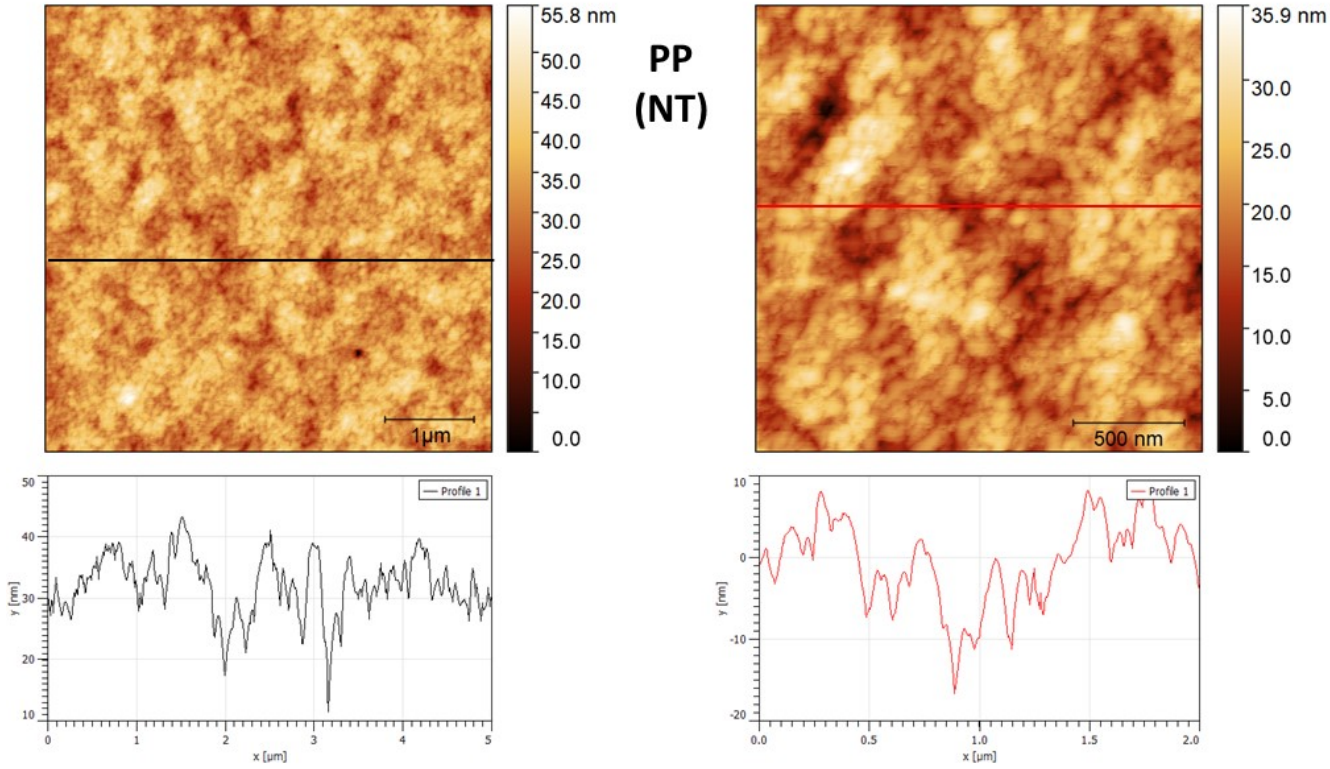

Figure S1b: The upper panels show the 2D topographic images for PP (NT) at two different scales, where the horizontal lines represent arbitrarily chosen cuts on the surface, whose linear profiles are displayed in the lower panels.

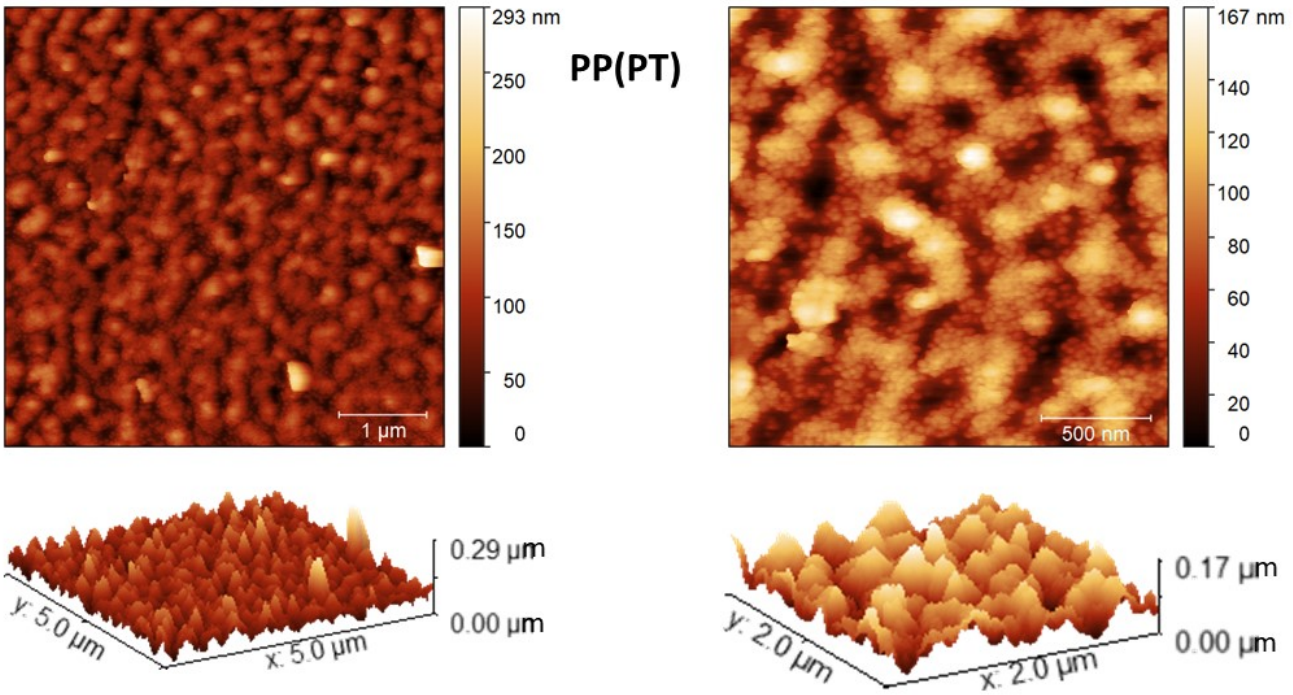

Figure S2a: Same as Figure S1a for PP (PT).

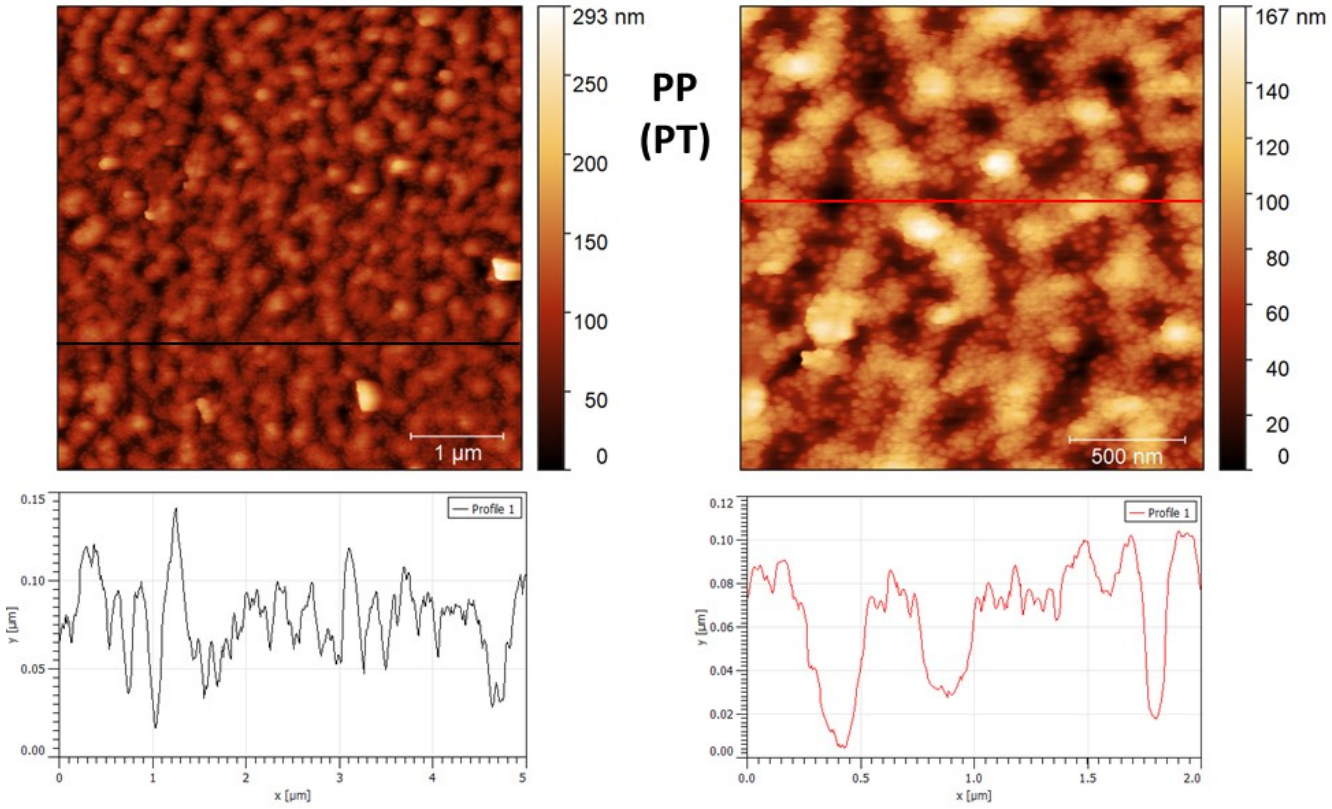

Figure S2b: Same as in Figure S1b for PP (PT).

In the following, we report in Figure S3 results for the 2D amplitude (left panels) and topographic (right panels) signal AFM images for both PP (NT) and PP (PT). The left images represent the variation in oscillation amplitude of the AFM probe while scanning the surface in tapping mode.

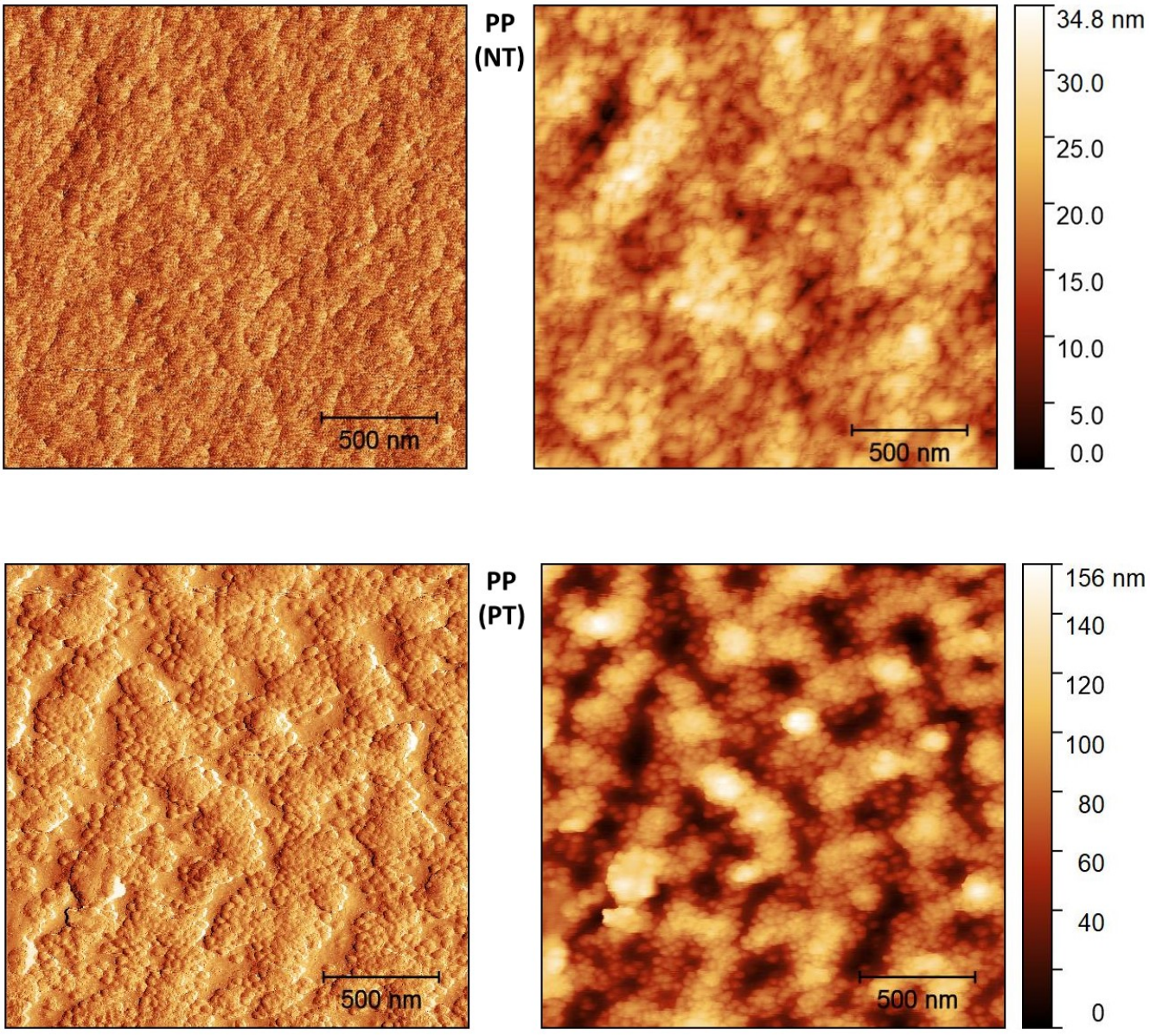

Figure S3: AFM amplitude (left panels) and topographic (right panels) images for PP (NT) and PP (PT).

(1.2) Polytetrafluoroethylene (PTFE)

The images for PTFE (NT), corresponding to Figure S1a, are shown in Figure S4a, while the plasma treated counterparts, corresponding to Figure S2a, are shown in Figure S4b.

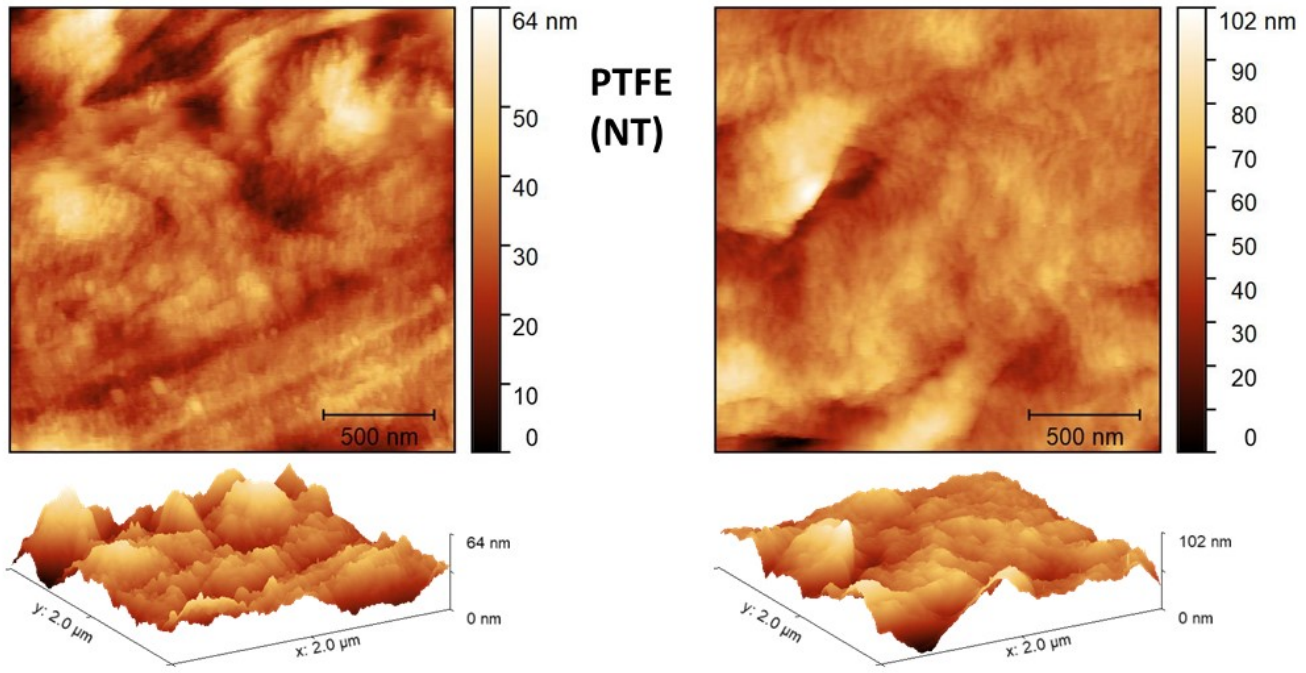

Figure S4a: Same as in Figure S1a for PTFE (NT). The RMS roughness is about 15 nm.

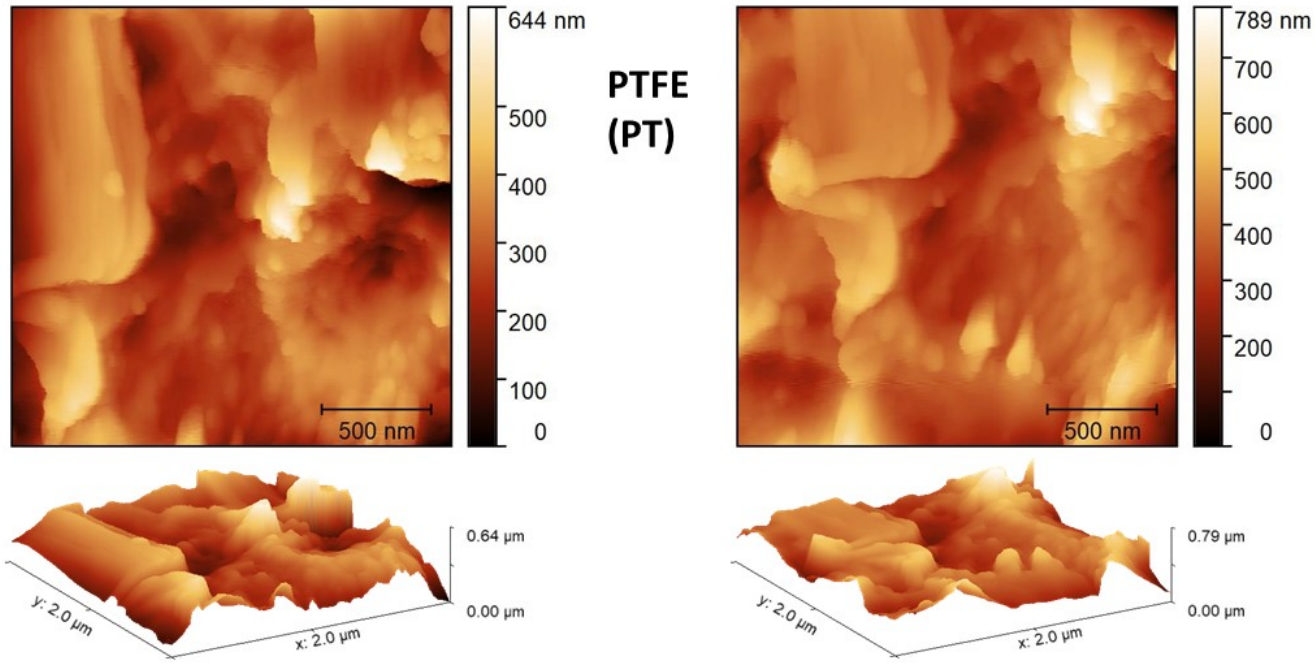

Figure S4b: Same as in Figure S1a for PTFE (PT). The RMS roughness is now about 100 nm.

The results of the amplitude variations in the case of PTFE, corresponding to Figure S3, are shown in Figure S5, for both NT and PT samples.

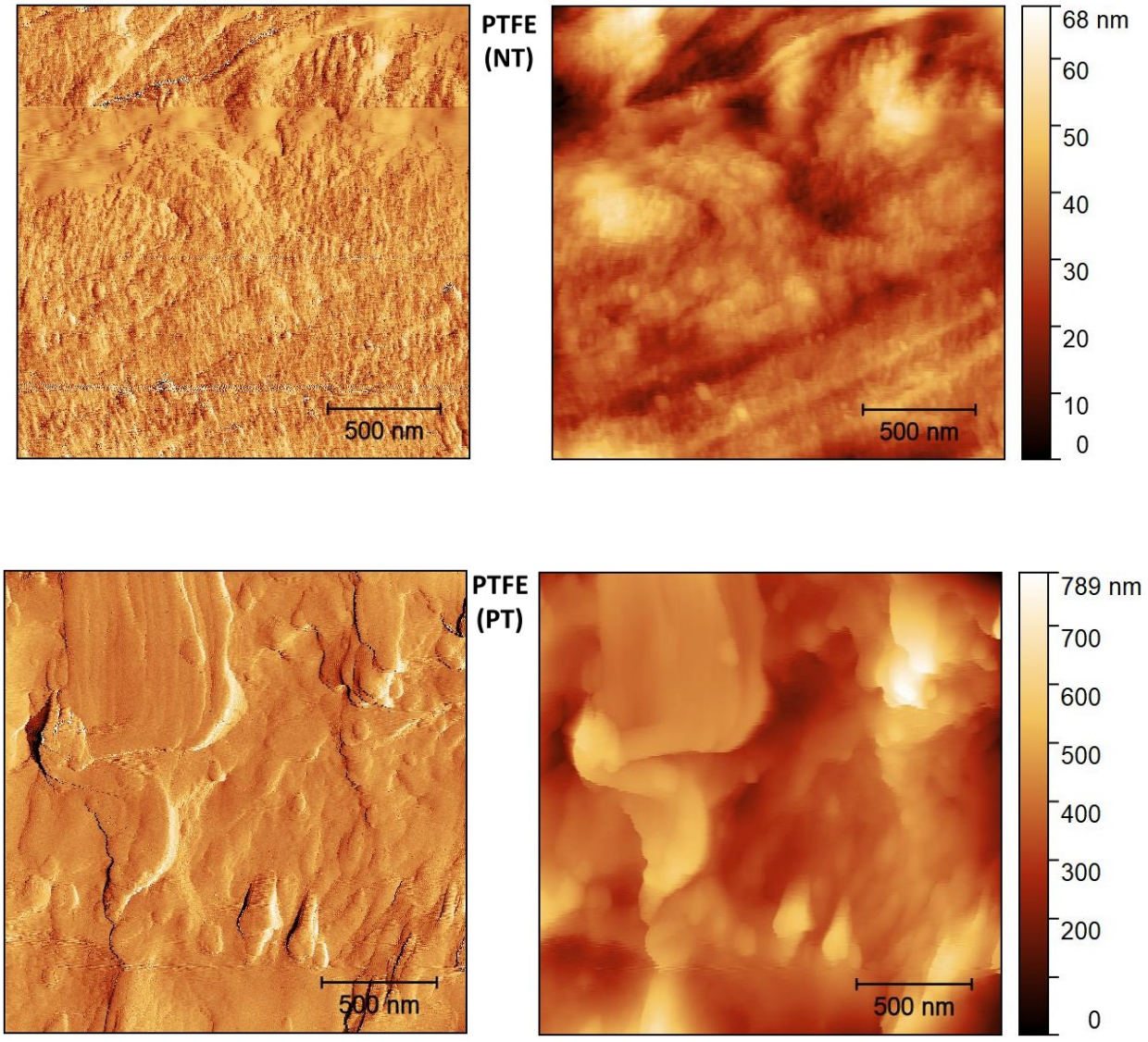

Figure S5: AFM amplitude (left panels) and topographic (right panels) images for PTFE (NT) and PTFE (PT).

(1.3) Polycaprolactone (PCL)

Same as in Figures S4a and S4b for PCL.

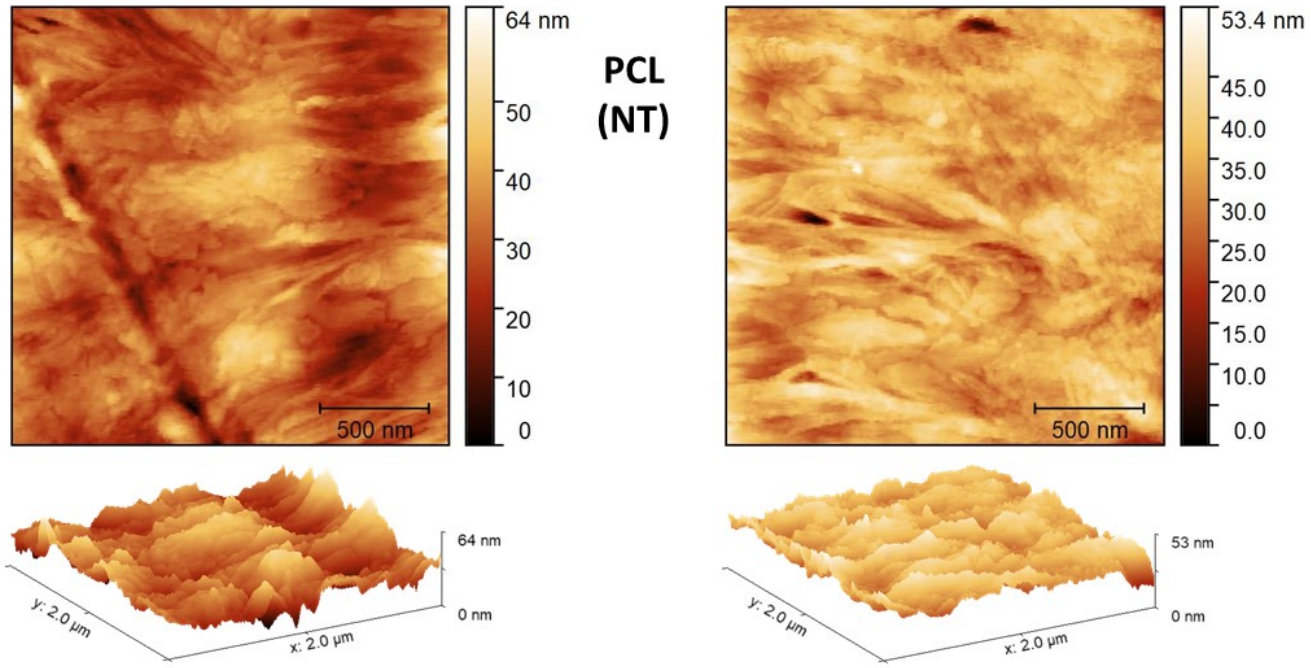

Figure S6a: Same as in Figure S4a for PCL (NT). The RMS roughness is about 10 nm.

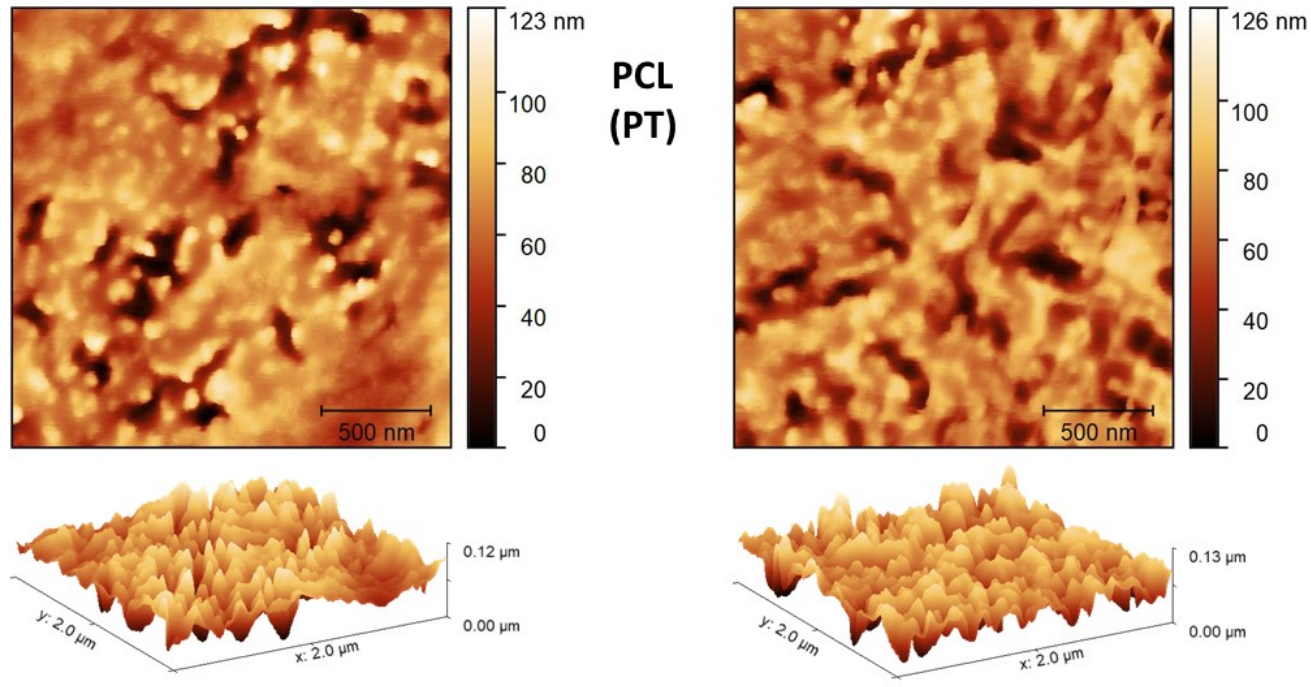

Figure S6b: Same as in Figure S4b for PCL (PT). The RMS roughness is about 20 nm.

The amplitude variations in the case of PCL, corresponding to Figure S3 and Figure S5, are shown in Figure S7, for both NT and PT samples.

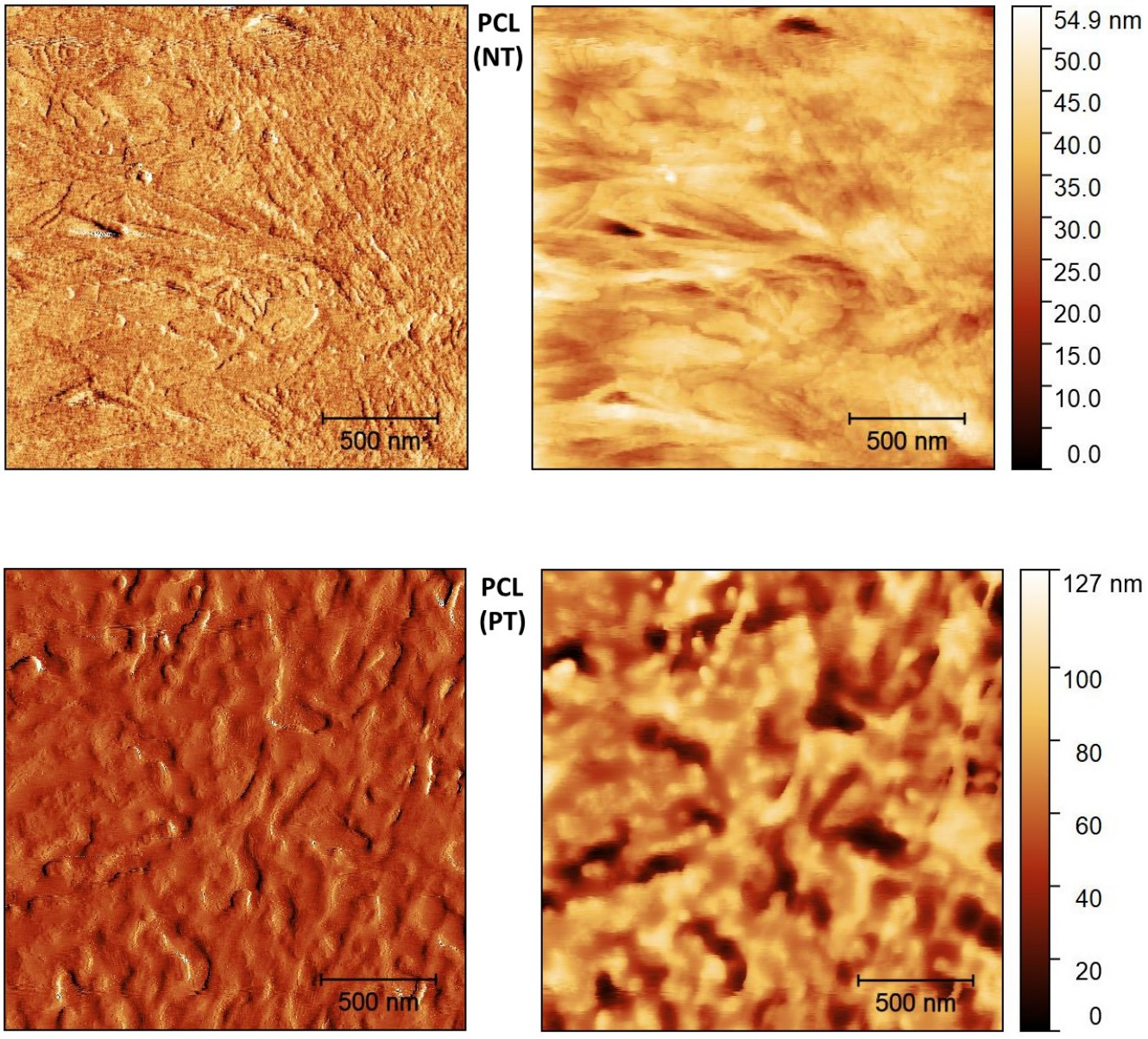

Figure S7: AFM amplitude (left panels) and topographic (right panels) images for PCL (NT) and PCL (PT).

(2) Scaling behaviour of NT and PT surfaces of PCL

In Figure S8 we show the AFM results for the PCL samples. The PCL surfaces seem to display scaling behavior closer to a flat surface than PP and PTFE materials. The average surface areas are: <A(NT)> ≃ 4.17 μm^2, i.e. ≃ 4.3% larger than the flat surface area 4 μm^2, while the plasma treated surface has <A(PT)> ≃ 4.98 μm^2, corresponding to a 25% relative increase in surface area. The scale-invariant range (S5e,f) is reduced considerably in this case, down to ≃ 50 nm.

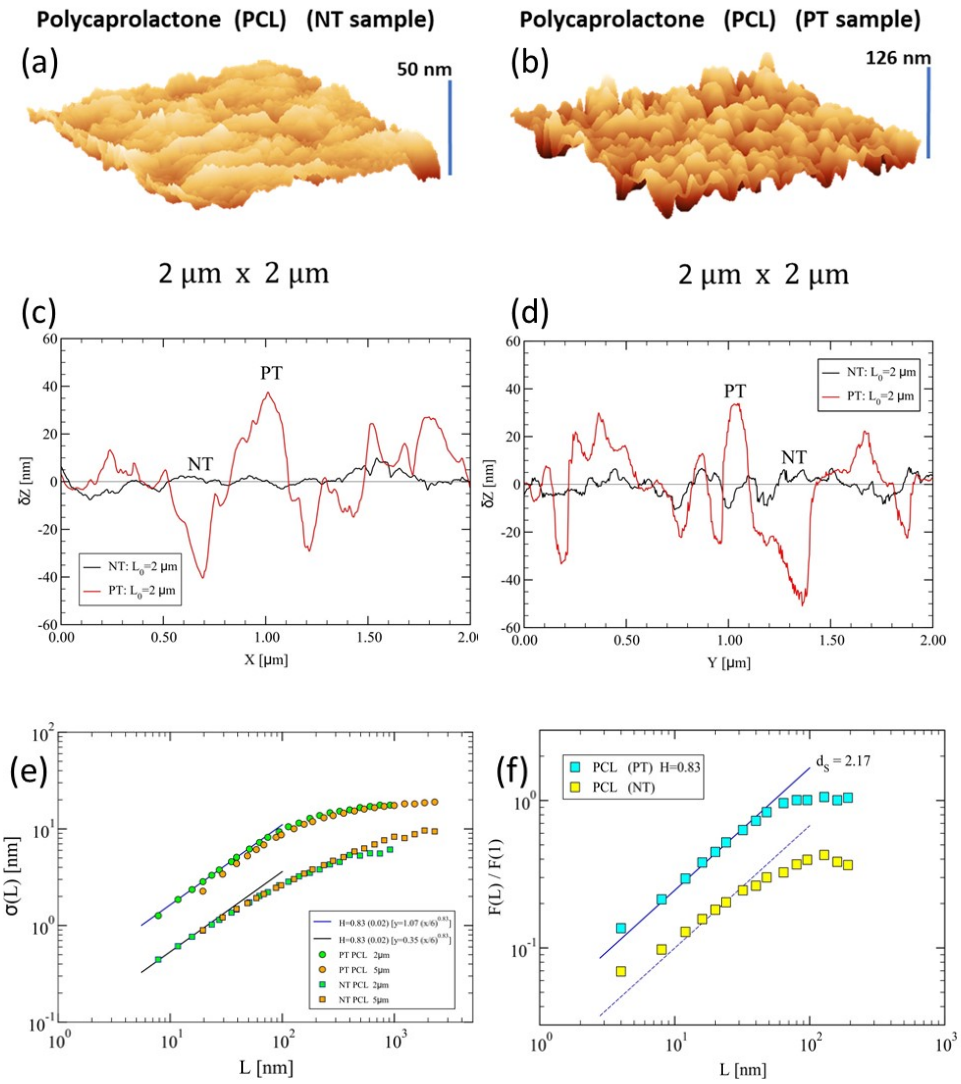

Figure S8: Same as in Figure 4, for Polycaprolactone (PCL) surfaces of 2μm x 2μm size. (**a**) The non-treated surface displays vertical fluctuations of amplitude Z ≃ 50 nm. (**b**) The plasma treated surface reaches higher fluctuations of about Z ≃ 126 nm. The AFM images have been obtained after 1 min of treatment. (**c**,**d**) Selected profile examples along x- and y-directions, respectively, for both NT and PT samples. (**e**) Scaling of amplitude fluctuations, σ(L), vs length scale L for PCL, yielding H = 0.83 ± 0.02 in both cases. Sample sizes are indicated in the inset. (**f**) Fluctuation analysis, F(L) / F(1) vs length scale L [nm], for surfaces of linear sizes L_0 = 2 μm. The straight line has slope H = 0.83 ± 0.02, yielding the fractal dimension, d_S = 2.17 ± 0.02, consistent with the value in (e). The dashed straight line has slope H = 0.83 and is included as a guide. The curves in (f) have been vertically shifted for clarity.

The scaling of amplitude fluctuations, Eq.(3), for PCL are shown in Figure S8e, and the fluctuation analysis in Figure S8f. Also here, both PT and NT samples display a similar fractal scaling at lower scales, however, on a reduced range of length scales, smaller than for PP and PTFE.

As once can see in Figures 8a and 8b, both surfaces (NT and PT) display strong height fluctuations, where the PT ones are larger by a factor of ≈3 w.r.t. the NT ones (cf. also Figures 8c and 8d). The actual fractal scaling are displayed in 8e (NT) and 8f (PT), showing similar power-law exponents, H. This result is surprising, and suggests that the non-treated surface has already developed an incipient fractal behavior. The latter seems to be typical of polymeric materials in more general cases, as we show in the paper for PP and PTFE materials. In other words, fractal scaling was already there, and the effect of the plasma treatment is to increase the fractal length scale. The following discussion holds also to the PP and PTFE cases.

To be noted is that real material surfaces are not exact fractals, but they 'appear' to obey power-law scaling on (always) a reduced (limited) range of length scales. The question is how to identify them 'correctly'. The rule of thumb says that we should look at intermediate length scales, i.e. not too long and not too short scales. There is always both a lower and an upper bound within which the data 'conforms' most accurately to a straight line (in a log-log plot), the slope of which is the fractal exponent. If one looks carefully at Figures 8e and 8f, one will notice that the straight lines are drawn according to this rule. Now, the NT sample displays a shorter range of length scales on which the power-law behaviour occurs. Also in Figure 8e we see that the amplitude of fluctuations for the PT sample are larger than for the NT one, that is both effects are present. The fact that the ranges are different in Figure 8e than in Figure 8f is due to the method of analysis used. Typically, F(L) is more accurate than the estimation of σ(L), but the trend in going from NT to PT is robust and it is clearly shown by the two methods.

The wetting properties of PCL are discussed in terms of the contact angle, as shown in Figure S9.

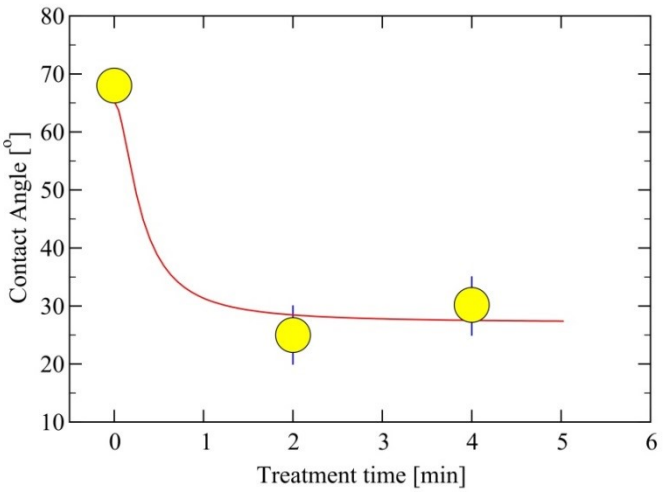

Figure S9: Contact angles of treated PCL surfaces vs treatment time, at 60W. The fit (continuous line) was obtained using Eq. (12) for the values: A = 0.89, B = 0.53, T_0 = 15 s, with d_S = 2.17 and H = 0.83. Some experimental error bars are indicated.

In the case of PCL, a very rapid decrease in contact angle, from ϑ_c = 68°C for the NT sample, down to $\vartheta_c \approx$ 30°C obtained after about 1 minute of treatment in oxygen plasma is found (Figure S9). The predictions of Eq. (12) are consistent with the experimental results.